

ORIGINAL ARTICLE

Downregulation of miRNA-31 induces taxane resistance in ovarian cancer cells through increase of receptor tyrosine kinase MET

T Mitamura^{1,2}, H Watari¹, L Wang², H Kanno², MK Hassan^{1,4}, M Miyazaki², Y Katoh², T Kimura², M Tanino², H Nishihara³, S Tanaka^{2,3} and N Sakuragi¹

Ovarian cancer is one of the most aggressive female reproductive tract tumors. Paclitaxel (PTX) is widely used for the treatment of ovarian cancer. However, ovarian cancers often acquire chemotherapeutic resistance to this agent. We investigated the mechanism of chemoresistance by analysis of microRNAs using the ovarian cancer cell line KFr13 and its PTX-resistant derivative (KFr13Tx). We found that miR-31 was downregulated in KFr13Tx cells, and that re-introduction of miR31 re-sensitized them to PTX both *in vitro* and *in vivo*. miR-31 was found to bind to the 3'-UTR of mRNA of MET, and the decrease in MET correlated to higher sensitivity to PTX. Furthermore, co-treatment of KFr13Tx cells with MET inhibitors sensitized the tumor cells to PTX both *in vitro* and *in vivo*. In addition, lower levels of miR31 and higher expression of MET in human ovarian cancer specimens were significantly correlated with PTX chemoresistance and poor prognosis. This study demonstrated miR31-dependent regulation of MET for chemoresistance of ovarian cancer, raising the possibility that combination therapy with a MET inhibitor and PTX will increase PTX efficacy.

Oncogenesis (2013) 2, e40; doi:10.1038/oncsis.2013.3; published online 25 March 2013

Subject Categories: molecular oncology

Keywords: ovarian cancer; microRNA; MET; chemoresistance; paclitaxel

INTRODUCTION

Ovarian cancer is the leading cause of death among malignancies of the female reproductive system, resulting in ~125 000 deaths annually.¹ Because of the wide variety of symptoms of ovarian cancer, most patients are in advanced stages (International Federation of Gynecology and Obstetrics (FIGO) stage III and IV) at the time of initial diagnosis,² and the 5-year overall survival rates are only 30–40%.^{3,4} The current therapy for ovarian cancer is debulking surgery followed by chemotherapy using carboplatin and paclitaxel (PTX).⁵ Although ovarian cancer in advanced stages initially appears to be chemotherapy sensitive as response rates to platinum-based therapy exceed 80%, long-term survival remains poor as a result of recurrence and emergence of drug resistance.

MicroRNAs (miRs) are endogenous non-coding RNAs of ~23-mer, which have important roles in regulation of gene expression. Mature form of miRs silence gene expression by binding to the 3'-UTR of target mRNAs and initiate translational repression or cleavage of cognate mRNAs.⁶ Following the initial demonstration of the important role for miR in human cancer, such as downregulation of miR-15a-miR-16-1 in chronic lymphocytic leukemia,⁷ a number of cancers have been shown to exhibit distinct miR expression patterns related to various phenotypes with remarkable cytogenetic abnormalities.^{8,9} Implication of miR in chemoresistance was reported in several cancers other than ovarian origin.^{10,11} Although there was a report for correlation of

miR, such as let7i, for chemoresistance of ovarian cancer,¹² the precise mechanism underlying the association is unknown.

In this study, we aimed to investigate the correlation between miR and sensitivity to PTX, and demonstrated that miR-31 was decreased in chemoresistant ovarian cancer. In addition, one of the direct targets of miR-31 was found to be receptor tyrosine kinase MET, and upregulation of MET caused the chemoresistance to PTX. These results suggest that MET inhibitors administered concurrently with PTX could prevent the development of resistance to PTX.

RESULTS

miR-31 was downregulated in ovarian cancer cells that acquired PTX resistance

To identify miRNAs that potentially cause the resistance to taxanes, such as PTX, we performed microarray analysis of miRNAs in KFr13 and PTX-resistant KFr13Tx cells. Fifty-five miRNAs were found to be downregulated below the half amount, while two miRNAs were upregulated more than twofold in KFr13Tx cells compared with wild-type KFr13. miRNAs that exhibited remarkable alterations are shown in Supplementary Table 1. Among these miRNAs, we focused on miRNA-31 (miR-31) because miR-31 was the only miR that has been reported to regulate tumor phenotype, an anti-metastatic effect in breast cancer.¹³ In fact,

¹Department of Obstetrics and Gynecology, Hokkaido University Graduate School of Medicine, Sapporo, Japan; ²Department of Cancer Pathology, Hokkaido University Graduate School of Medicine, Sapporo, Japan and ³Department of Translational Pathology, Hokkaido University Graduate School of Medicine, Sapporo, Japan. Correspondence: Associate Professor H Watari, Department of Obstetrics and Gynecology, Hokkaido University Graduate School of Medicine, N15, W7, Kita-ku, Sapporo, Hokkaido 060-8638, Japan. E-mail: watarih@med.hokudai.ac.jp or Associate Professor H Nishihara, Department of Translational Pathology, Hokkaido University Graduate School of Medicine, N15, W7, Kita-ku, Sapporo, Hokkaido 060-8638, Japan. E-mail: hnishihara@s5.dion.ne.jp or Professor S Tanaka, Department of Cancer Pathology, Hokkaido University Graduate School of Medicine, N15, W7, Kita-ku, Sapporo, Hokkaido 060-8638, Japan. E-mail: tanaka@med.hokudai.ac.jp

⁴Current address: Biotechnology program, Zoology Department, Faculty of Science, PS U; Port Said University, Port Fouad, Port Said, Egypt.

Received 29 January 2013; accepted 3 February 2013

miR-31 was negatively correlated with IC50 values of PTX between six cell lines including KFr13, RMG-1, SK-OV-3, OVCAR-3, KF and TU-OM-1 (Figure 1a).

Overexpression of miR-31 re-sensitized PTX-resistant ovarian cancer cells to PTX *in vitro*

To confirm the results of array analysis in which levels of miR-31 was decreased in PTX-resistant cells, quantitative real-time PCR analysis was performed, and as expected, the levels of miR-31 was significantly suppressed in KFr13Tx cells (Figure 1b). To assess the biological role of miR-31, we next tried to establish ovarian cancer cells overexpressing miR-31 by introducing pre-miR31 using lentivirus vectors. We used KFr13Tx cells because miR-31 was substantially decreased in KFr13Tx when it acquired PTX resistance among several cell lines mentioned above and lentivirus vector was efficiently transfected in this cell line. Finally, we established KFr13Tx cells overexpressing three different levels of miR-31 designated as KFr13Tx miR-31(1), miR-31(2) and miR-31(3) (Figure 1c), and performed MTT assays to evaluate the sensitivity to PTX. After incubation with 500 nM of PTX for 72 h, we found that the ovarian cancer cells with higher amounts of miR-31 exhibited lower cell viability (Figure 1d). Conversely, inhibition of miR-31 expression in KFr13 cells by oligonucleotides increased cell viability after incubation with 500 nM PTX for 48 h (Figure 1e). It is notable that miR-31 introduction did not change the sensitivity to other agents such as carboplatin, irinotecan, doxorubicin and gemcitabine in KFr13Tx (Supplementary Table 2). These results suggested that the decrease of miR-31 caused PTX-specific resistance in KFr13.

miR-31 reduced protein levels of MET through the inhibition of translation

To elucidate the mechanism by which miR-31 regulates PTX sensitivity, *in silico* prediction models were employed to identify the target mRNA of miR-31 for chemosensitivity in ovarian cancer⁶ (Supplementary Table 3). Among these targets, we focused on receptor tyrosine kinase MET because one potential binding site for miR-31 was found in 3'-UTR of MET mRNA (Supplementary Figure S1a). To ensure that MET is a *bona fide* target of miR-31, RNA fragments that bind to Ago2 were analyzed, and the 3'-UTR region of MET was found to be isolated from the Ago2-dependent immunoprecipitated RNA fraction of KFr13Tx miR-31 cells (Figure 2a). For further confirmation, the protein levels of MET was analyzed in KFr13 cells overexpressing miR-31, and we found that MET was downregulated in miR31-overexpressing cells in a dose-dependent manner (Figure 2b). As expected, the expression level of MET was increased in KFr13Tx cells compared with that in KFr13 cells (Figure 2b). Conversely, an increase of MET protein levels was observed after introduction of anti-miR-31 oligonucleotides into KFr13 cells (Supplementary Figure S1b). The same tendency that ovarian cancer cells with higher miR-31 showed lower MET expression was also observed in other cell lines used in the PTX sensitivity experiment mentioned above. Expression of MET was extremely low in RMG-1 and relatively low in SK-OV-3, OVCAR-3 and KFr13, and high in KF and TU-OM-1, both of which were resistant to PTX and expressed low miR-31 (Figure 2c). Subsequently, we analyzed the mechanism by which miR-31 regulates endogenous protein levels of MET, focusing on transcriptional or translational regulation. As no significant difference of MET mRNA was observed between KFr13 and KFr13Tx cells (Figure 2d), miR-31 did not seem to inhibit transcription. On the other hand, when translation was inhibited by CHX, levels of MET were decreased, suggesting translational regulation of MET by miR-31, although a decrease in MET levels in the presence of CHX does not necessarily demonstrate a direct translational regulation of MET by miR-31, as the suppressive effect by CHX on translation is nonspecific and may inhibit

expression of various proteins including those affecting the regulation of MET levels. The levels of MET were low in spite of the presence or absence of CHX in case of miR31-overexpressing cells (Supplementary Figure S1c).

To ensure that MET mRNA is a target of miR-31, we utilized a luciferase reporter assay. Normalized luciferase activity revealed that miR-31 significantly suppressed the activity of luciferase combined with wild-type MET 3'-UTR in KFr13Tx miR-31 cells, whereas no difference was observed with the control luciferase vector (Figure 2e). Furthermore, miR-31 did not affect luciferase with MET 3'-UTR possessing a mutation in the putative miR-31-binding site in KFr13Tx miR-31. These results suggest that miR-31 directly suppressed the protein expression of MET *via* sequence-specific interactions with 3'-UTR of MET mRNA.

As MET was reported to be degraded by the ubiquitin-proteasome pathway,¹⁴ we utilized a proteasome inhibitor, MG132, to exclude the possibility that miR-31 indirectly regulates protein levels of MET through a ubiquitin-dependent protein degradation mechanism. After treatment with MG132 for 4 h, MET expression in KFr13Tx miR-31 was not altered by inhibition of proteasome function, while the amount of p53 was increased as positive control for ubiquitin-dependent protein degradation¹⁵ (Supplementary Figure S1d). These results suggest that miR-31 directly binds to MET mRNA and regulates MET expression by translational inhibition.

MET contributes to PTX resistance of ovarian cancer cells

To investigate whether MET is responsible for the resistance of KFr13Tx cells to PTX, expression of MET was suppressed by three different small interfering RNAs (siRNAs) (Figure 3a, bottom) and the treated cells were evaluated for chemosensitivity by the MTT assay. After incubation with 500 nM of PTX for 72 h, significantly lower viability was observed in cells with MET suppression, whereas nonspecific siRNA did not affect the viability of KFr13Tx cells (Figure 3a, top). These results suggest that MET contributes to chemoresistance to PTX in ovarian cancer cells.

Based on our results suggesting the presence of MET-dependent chemoresistance, we explored molecular-targeting treatments to determine whether MET inhibitors could re-sensitize resistant tumors to PTX. Two different MET kinase inhibitors, SU11274 and PHA665752, were utilized at the concentration with minimum effect on viability of KFr13Tx mock cells (Figure 3b, lanes 1 and 2). At this concentration, the protein levels of phospho-MET and phospho-Akt were significantly decreased (Figure 3b bottom). After incubation with MET inhibitors together with PTX, the KFr13Tx cells were sensitive to PTX. Furthermore, even in the presence of HGF stimulation, MET inhibitors reversed the chemoresistance to PTX in KFr13Tx cells (Supplementary Figure S2). Based on these results, we concluded that the downregulation of miR-31 induced chemoresistance of ovarian cancer cells to PTX through the upregulation of MET *in vitro*.

Overexpression of miR-31 re-sensitized PTX-resistant ovarian cancer cells to PTX *in vivo*

To investigate the effects of miR-31 on PTX sensitivity *in vivo*, we examined a murine xenograft tumor model. KFr13Tx mock or miR-31 were injected subcutaneously into the flank of mice, and chemosensitivity of the tumors was evaluated. Without PTX treatment, the weight of the tumors was similar in mock and miR31-overexpressing KFr13 cells. In contrast, under treatment with PTX, miR31-overexpressing tumors were significantly smaller than that of mock expressing tumors (Figure 4a, top). Consistent with the smaller tumor size, mice harboring miR31-overexpressing tumor survived longer during the treatment with PTX (Figure 4a, bottom). The weights of subcutaneous tumor nodules derived from drug-resistant KFr13Tx mock cells were reduced by the combination of MET inhibitor SU11274 with PTX (Figure 4b, top).

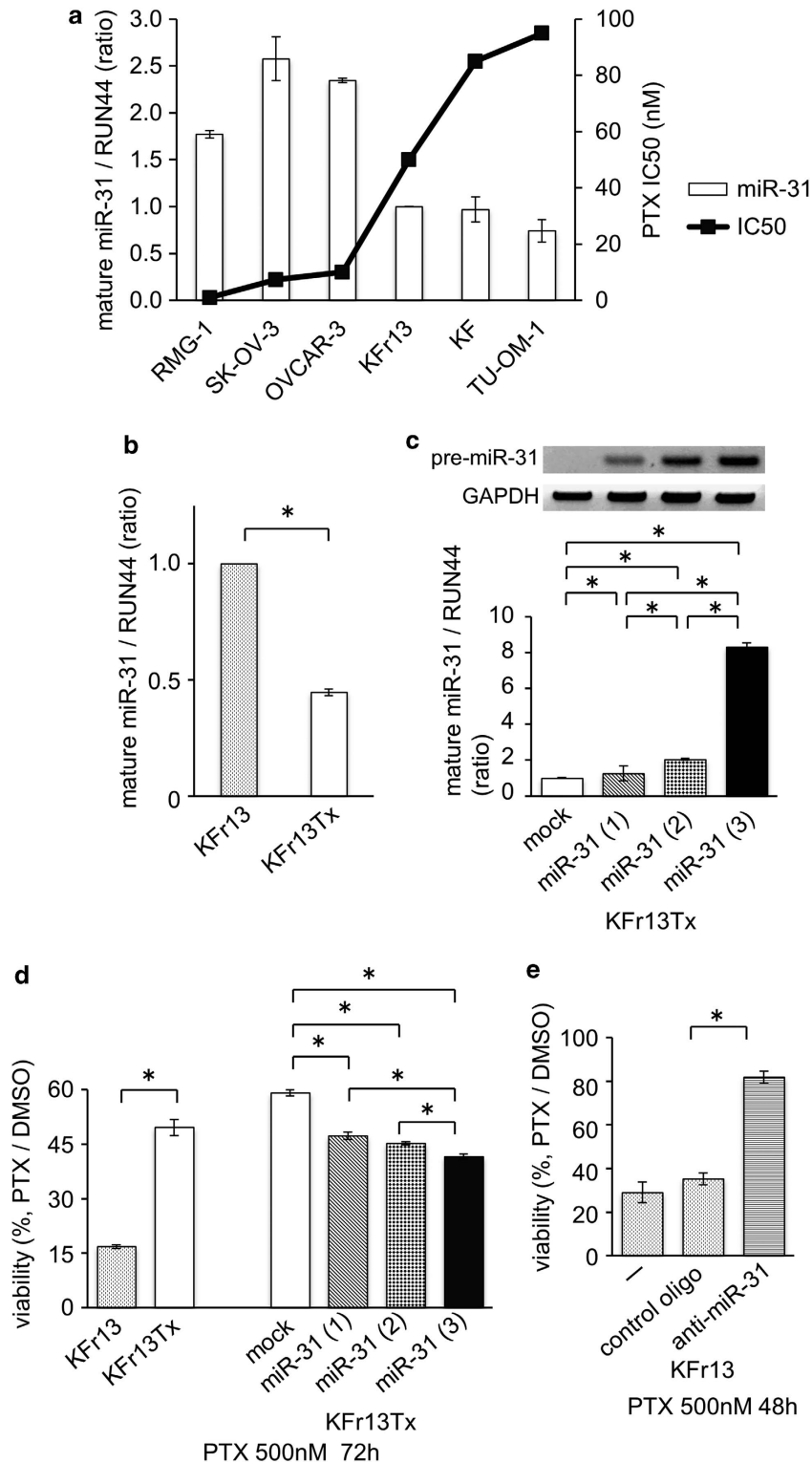
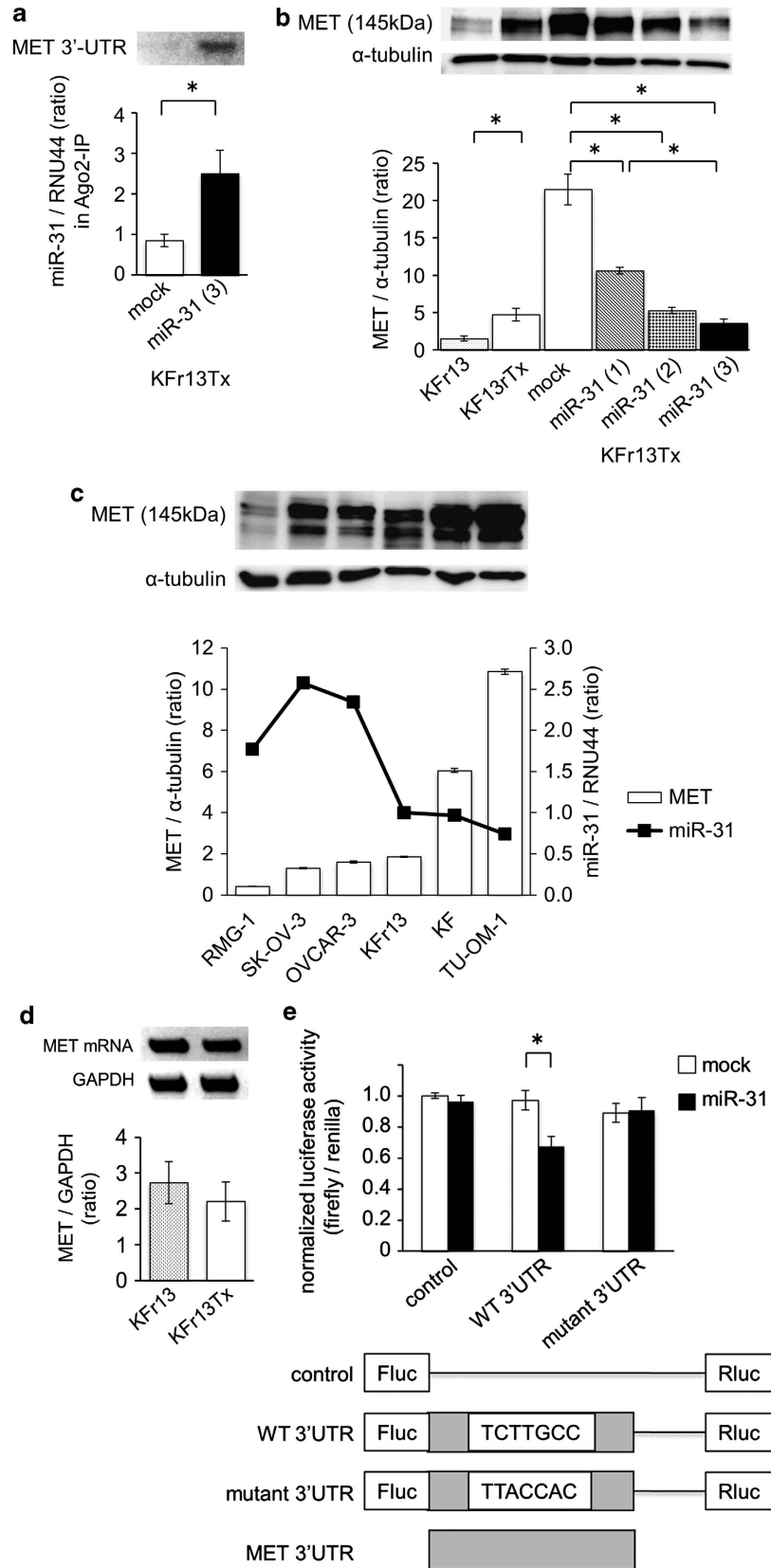


Figure 1. Overexpression of miR-31 re-sensitized PTX-resistant ovarian cancer cell to PTX *in vitro*. **(a)** Real-time PCR analysis of expression levels of miR-31 and IC₅₀ of PTX in six human ovarian cancer cell lines. **(b)** Real-time PCR analysis of expression levels of miR-31 in parental (KFr13) and PTX-resistant (KFr13Tx) cells. **P* < 0.05. **(c)** Establishment of three cell lines of KFr13Tx expressing miR-31. Expression levels of miR-31 in cells named as miR-31 (1), miR-31 (2) and miR-31 (3) are low, middle and high, respectively. Representative RT-PCR bands are shown as top panel. Real-time PCR analysis of expression levels of miR-31 in miR-31 (1), miR31 (2) and miR (3) are shown in bottom bar graph. Original gel is presented in Supplementary Figure S3a, **P* < 0.05. **(d)** Chemosensitivity to PTX is shown by MTT assay, **P* < 0.05. **(e)** Effect of anti-miR-31 on chemosensitivity to PTX analyzed by MTT assay, **P* < 0.05.



Furthermore, overall survival of the mice with the KFr13Tx mock tumors was found to be improved by the combination treatment of MET inhibitor with PTX (Figure 4b, bottom). These results suggest that the combination of PTX and SU11274 may be an option for the treatment of ovarian cancer refractory to PTX.

Lower expression levels of miR-31 and higher levels of MET in human ovarian cancer specimens are associated with chemoresistance

To explore the relevance of our findings to the clinic, we analyzed the expression levels of miR-31 in surgical specimens from human ovarian cancer patients (Table 1). We needed to investigate the patients with measurable target lesions in advanced-stage cancer, namely with suboptimal resection, to examine the correlation between chemosensitivity and miR-31 expression and selected

the patients with serous adenocarcinomas that usually show advanced-stage disease.¹⁶ All 12 cases were women with serous adenocarcinomas with FIGO Stage IIIc or IV,¹⁶ who underwent surgery as their initial treatment. As the initial surgery was suboptimal in all patients, the subjects were stratified by response to subsequent chemotherapy (more than three courses in all cases) according to the Response Evaluation Criteria in Solid Tumors (RECIST version1.1).¹⁷

The 12 tumors were divided into two groups, sensitive and resistant, based on the response to chemotherapy. We found that the expression levels of miR-31 were lower in resistant tumors compared with sensitive ones (Figure 5a). Moreover, the lower expression of miR-31 strongly correlated with reduced overall survival in Stage IIIc patients, who were treated with PTX and carboplatin (Figure 5b). In agreement with our *in vitro* data, the higher protein levels of MET were correlated with lower levels of miR-31 in the cohort analysis of the tumors (Figure 5c). These data

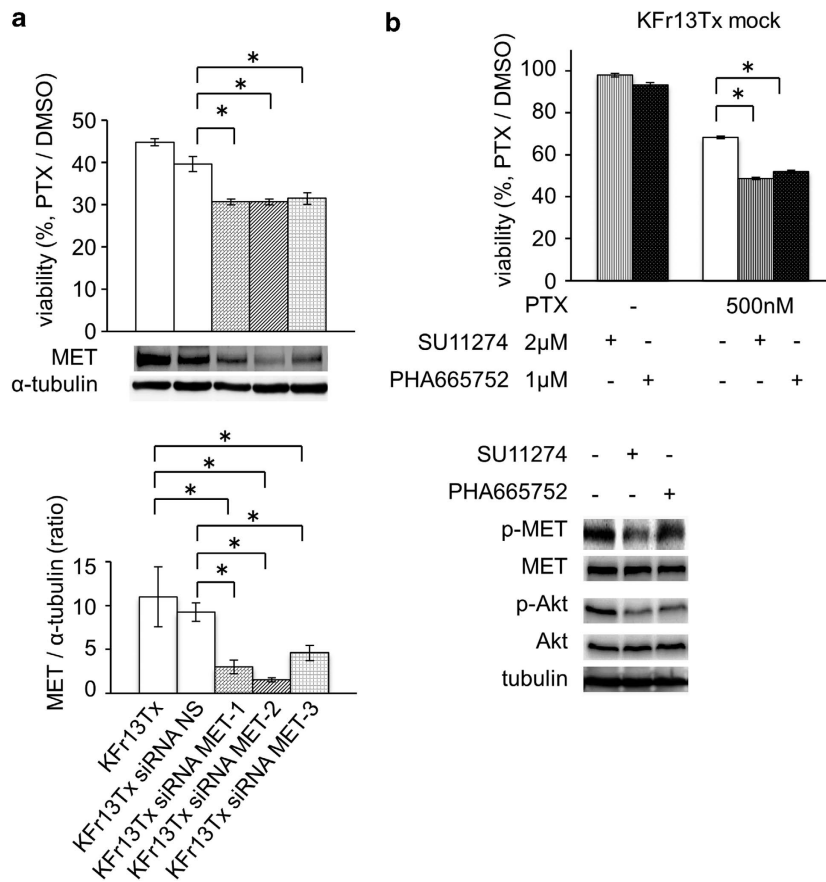


Figure 3. MET regulates PTX sensitivity in ovarian cancer cell *in vitro*. (a) Chemosensitivity to PTX of KFr13Tx analyzed by MTT assay are shown as bar graph (top). Immunoblotting of MET and α -tubulin when siRNAs were transfected (middle panel). The ratio of MET/ α -tubulin is shown as bar graph (lower). Original blots are presented in Supplementary Figure S3e, * $P < 0.05$. (b) Effect of MET inhibitor, SU11274 and PHA665752 on chemosensitivity to PTX analyzed by MTT assay. Effect of MET inhibitor was validated by immunoblotting for phosphorylated form of MET (pMET) and Akt (pAkt). Original blots are presented in Supplementary Figure S3f, * $P < 0.05$.

Figure 2. miR-31 regulates MET expression by translation inhibition. (a) Detection of MET mRNA by RT-PCR (top panel) and miR-31 by real-time PCR in Ago2-mediated immunoprecipitated RNA fraction in KFr13Tx. Original gel is presented in Supplementary Figure S3b, * $P < 0.05$. (b) Expression levels of MET in wild-type and miR31-overexpressing cells. Results of immunoblotting of MET and α -tubulin are shown as top panel and the ratio of MET/ α -tubulin are shown as bar graph. Original blots are presented in Supplementary Figure S3c, * $P < 0.05$. (c) Expression levels of MET and miR-31 in six human ovarian cancer cell lines. Results of immunoblotting of MET and α -tubulin are shown as top panel. The ratio of MET/ α -tubulin and miR-31 expression is shown in bottom bar and line graph, respectively. (d) mRNA levels of MET in KFr13 and KFr13Tx analyzed by RT-PCR are shown as top panel. Ratio of MET/GAPDH is shown as bar graph. Original gel is presented in Supplementary Figure S3d. (e) Luciferase activity after transfection of the indicated 3'-UTR-driven reporter constructs. Reporter plasmid containing 3'-UTR region of MET as WT3'-UTR and its mutant as mutant 3'-UTR, * $P < 0.05$.

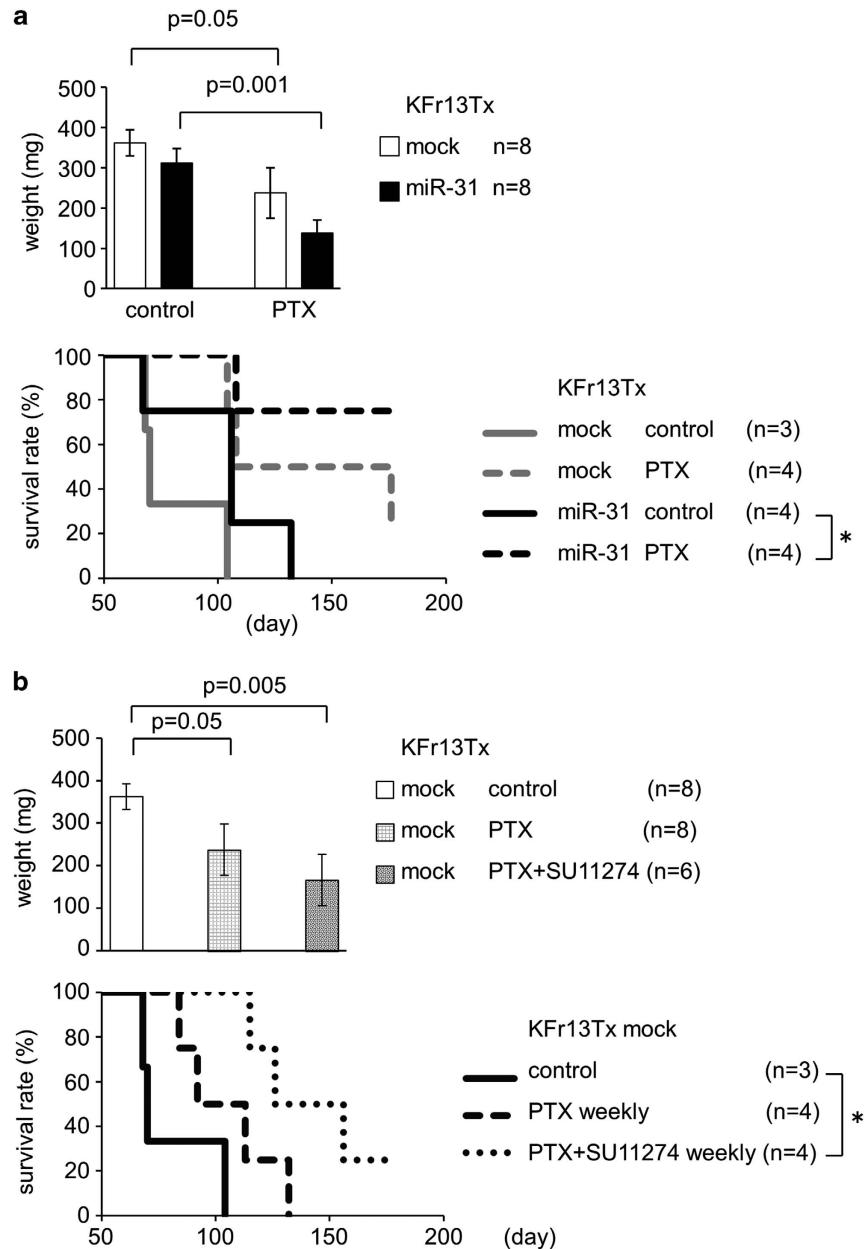


Figure 4. (a, top graph) Overexpression of miR-31 re-sensitized PTX-resistant ovarian cancer cell to PTX *in vivo*. Average of the weight of tumor in flank of mice. Solid bar indicates miR-31-expressing KFr13Tx cells. Open bar indicates KFr13Tx cells. Unpaired one-tailed *t*-test. (a, bottom graph) Survival of mice with intraperitoneal injection of KFr13Tx or KFr13Tx expressing miR-31 treated with PTX. KFr13Tx with PTX (gray broken line), KFr13Tx without PTX (gray solid line), KFr13Tx expressing miR-31 with PTX (black broken line), KFr13Tx expressing miR-31 without PTX (black solid line). * $P < 0.05$, log-rank test. (b, top graph) Effect of combination treatment of MET inhibitor and PTX on KFr13Tx cells *in vivo*. Average of the weight of tumor in flank of mice. Open bar indicates no treatment, closed bar as PTX alone, hatched bar as combination of both PTX and MET inhibitor SU11274. * $P < 0.05$, unpaired one-tailed *t*-test. (b, bottom graph) Survival of mice with intraperitoneal injection of KFr13Tx with no treatment, PTX alone, and both PTX and SU11274. Kaplan–Meier curves, * $P < 0.05$, log-rank test.

suggest the levels of miR-31 may predict the response to standard chemotherapy in ovarian cancer and serve as a prognostic factor.

DISCUSSION

The survival rate of early ovarian cancer is good and the outcome of early-stage disease might largely depend on the surgical factor, that is, the complete resection of tumors. On the other hand, the prognosis of the patients with optimally resected stage III–IV ovarian cancer is also known to be relatively good. However, when there are residual tumors of a size more than the greatest

dimension of 1 cm, the prognosis of those patients largely depends on chemosensitivity, because complete resection of the residual tumors will be possible when chemotherapy is effective.¹⁸ As ovarian cancer is usually undetected until it reaches an advanced stage, ~50–60% of patients gain no improvement in their prognosis from cytoreductive surgery.¹⁹ However, there is a certain population of women who have disease that is highly responsive to chemotherapy with PTX after suboptimal surgical ablation and who achieve a long survival.

In this study, we aimed to identify markers that identify chemotherapy responder patients by the comparing characteristics of

Table 1. Chemosensitivity and clinical features of human ovarian cancer

| Case | Age | Histology | FIGO stage | Primary debulking surgery | Response to chemotherapy | Regimen |
|------------------|-----|-----------|------------|---------------------------|--------------------------|---------|
| <i>sensitive</i> | | | | | | |
| 1 | 42 | serous | IIIc | suboptimal | PR | TC |
| 2 | 47 | serous | IIIc | suboptimal | PR | TC |
| 3 | 47 | serous | IIIc | suboptimal | PR | TC |
| 4 | 52 | serous | IIIc | suboptimal | PR | TC |
| 5 | 51 | serous | IV | suboptimal | CR | TC |
| 6 | 66 | serous | IV | suboptimal | PR | TC |
| <i>resistant</i> | | | | | | |
| 7 | 38 | serous | IIIc | suboptimal | SD | TC |
| 8 | 53 | serous | IIIc | suboptimal | SD | DC |
| 9 | 54 | serous | IIIc | suboptimal | SD | TC |
| 10 | 67 | serous | IIIc | suboptimal | PD | TC |
| 11 | 52 | serous | IV | suboptimal | SD | TC |
| 12 | 51 | serous | IV | suboptimal | PD | DC |

Abbreviations: CR, complete response; DC, docetaxel + carboplatin; PD, progressive disease; PR, partial response; SD, stable disease; TC, paclitaxel + carboplatin. Suboptimal, > 1 cm of residual disease.

chemosensitive and chemoresistant ovarian cancer cells. We discovered that tumor miR-31 expression levels might be a useful marker of chemotherapy response. In addition, we also demonstrated that MET is one of the targets of miR-31, whose overexpression is responsible for chemoresistance. Moreover, we provide evidence that poor responders might be rescued by a combination of standard chemotherapy with inhibitors for MET.

PTX is thought to dysregulate tubulin polymerization and microtubule formation,²⁰ inhibiting cell cycle and mitosis resulting in apoptosis of tumor cells.²¹ Previously, several mechanisms for development of PTX resistance have been reported.^{22–26} Amplification and increased expression of MDR1-encoded phosphoglycoprotein (PGP), which belongs to the superfamily of ATP-binding cassette (ABC) transporters, promotes efflux of anticancer drugs such as PTX.²⁷ It is noteworthy that one of these transporters, ABCB9, was a candidate target of miR-31, but protein expression levels of ABCB9 were similar between KFr13Tx mock and KFr13Tx expressing miR-31 (data not shown). The detailed molecular mechanisms that may contribute to drug resistance in ovarian cancers are still not fully understood, and new therapeutic strategies to overcome drug resistance need to be established.⁵

Recently, versatile roles for miRs have been identified in various human cancers⁹ and there are several reports about the correlation between miRs and chemoresistance. Upregulation of miR-125b and repression of its direct target Bak1 inhibited PTX-induced apoptosis in breast cancer.¹⁰ miR-199a-3p increased doxorubicin sensitivity of human hepatocarcinoma cells by repressing mTOR.¹¹ miR-21 induced resistance to 5-fluorouracil by downregulating human DNA MutS homolog2 (hMSH2) in colorectal cancer cells, and reducing G2/M arrest and apoptosis following exposure to 5-fluorouracil.²⁸ These reports suggest that miRs are potential targets for the development of novel approaches for cancer treatment. In this study, we compared the profiles of miRs between PTX-resistant and their chemosensitive parental cells, and demonstrated a role for miR-31 in ovarian cancer chemoresistance. Thus, miR profiling and the identification of miR targets is a fruitful approach to identify the molecular basis of cancer cell phenotypes.

It should be noted that, beside miR-31, the levels of several cancer-related miRs^{29,30} were also significantly altered in the acquisition of chemoresistance (Supplementary Table S1). Thus, miR-31 may not be the only miR regulating the malignant

potential of ovarian cancer. Based on our findings, we can conclude that miR-31 is involved at least in PTX resistance of ovarian cancers. Other studies have suggested that miR-221, miR-181b and miR-181d induce tamoxifen resistance in breast cancer, S-1 resistance in colon cancer and docetaxel-induced multidrug resistance in head and neck squamous cell cancer, respectively.^{30–32} Therefore, there may be tissue specificity for miRs in terms of chemoresistance in various different cancers.

In this present study, we have focused on miR-31 and our data represent the first demonstration of miR-31-mediated chemoresistance. However, it should be noted that miR-31 might have other roles associated with human cancers. Overexpression of miR-31 inhibits cancer cell proliferation by p53-dependent mechanisms in ovarian cancer cells.³³ miR-31 was also reported to inhibit metastasis, while it enhanced primary tumor growth of breast cancer.¹³ Furthermore, there is a report suggesting that miR-31 inhibits cell proliferation, migration and invasion in malignant mesothelioma.³⁴ Contributions of miR-31 to the activation of hypoxia-inducible factor for development of head and neck squamous cell cancer were also described.³⁵ Considering these reports, the roles of miR-31 in tumor cell proliferation and metastasis are complex.

The HGF receptor tyrosine kinase MET was originally isolated as oncogene product and is well known to possess versatile roles in cells including cancer cell invasion, motility and growth.³⁶ Recent studies have highlighted the effects of MET inhibitors on lung cancer with mutations of EGFR and amplification of MET.^{37,38} MET has been shown to mediate apoptotic resistance to therapeutic drugs in case of ovarian cancer through the activation of a PI-3 kinase-/AKT-dependent mechanism.^{39,40} Multikinase inhibitors suppressing MET and VEGFR activity have been reported to inhibit proliferation and metastasis of ovarian cancer.⁴¹ Together with the report that MET was frequently expressed in ovarian cancers, and elevated levels of MET correlate with lower overall survival,⁴² our results suggest that concurrent use of MET inhibitor with conventional anticancer drugs may improve outcomes for ovarian cancer patients.

In conclusion, the present study suggests that downregulation of miR-31 induces resistance of ovarian cancer to taxanes like PTX through upregulation of MET. Our findings provide a basis for clinical studies to determine if miR-31 expression levels are a marker of chemosensitivity in ovarian cancer patients, and if MET kinase inhibitors can rescue the PTX response in women with chemoresistant ovarian cancers.

MATERIALS AND METHODS

Cell lines

Human KF ovarian cancer cells and KFr13 cisplatin-resistant KF ovarian cancer cells were kindly provided by Prof Yoshihiro Kikuchi (National Defense Medical College, Saitama, Japan).⁴³ SK-OV-3 and OVCAR-3 were obtained from the ATCC (Manassas, VA, USA). RMG-1 was obtained from Health Science Research Resources Bank (Osaka, Japan). TU-OM-1⁴⁴ was kindly provided by Dr Junzo Kigawa (Tottori University School of Medicine). KFr13, KF were maintained in RPMI 1640 with 10% fetal bovine serum (FBS), 2 mM L-glutamine and 100 U/ml penicillin and streptomycin. To establish PTX-resistant KFr13 (KFr13Tx), cells were cultured with 2 nM of PTX, then the PTX concentration was gradually increased to 30 nM. SK-OV-3 was maintained in McCoy's 5a Medium Modified with 10% FBS, 2 mM L-glutamine and 100 U/ml penicillin and streptomycin. OVCAR-3 was maintained in RPMI 1640 with 20% FBS, 0.01 mg/ml bovine insulin, 2 mM L-glutamine and 100 U/ml penicillin and streptomycin. TU-OM-1 was maintained in Dulbecco's modified eagle's medium with 10% FBS, 2 mM L-glutamine and 100 U/ml penicillin and streptomycin.

Reagents and measurement of drug sensitivity by MTT assay

PTX, irinotecan (Sigma, St Louis, MO, USA), MET kinase inhibitors, such as SU11274 (Merckmillipore, Darmstadt, Germany), PHA665752 (Santa Cruz Biotechnology, Dallas, TX, USA), epidermal growth factor receptor inhibitor

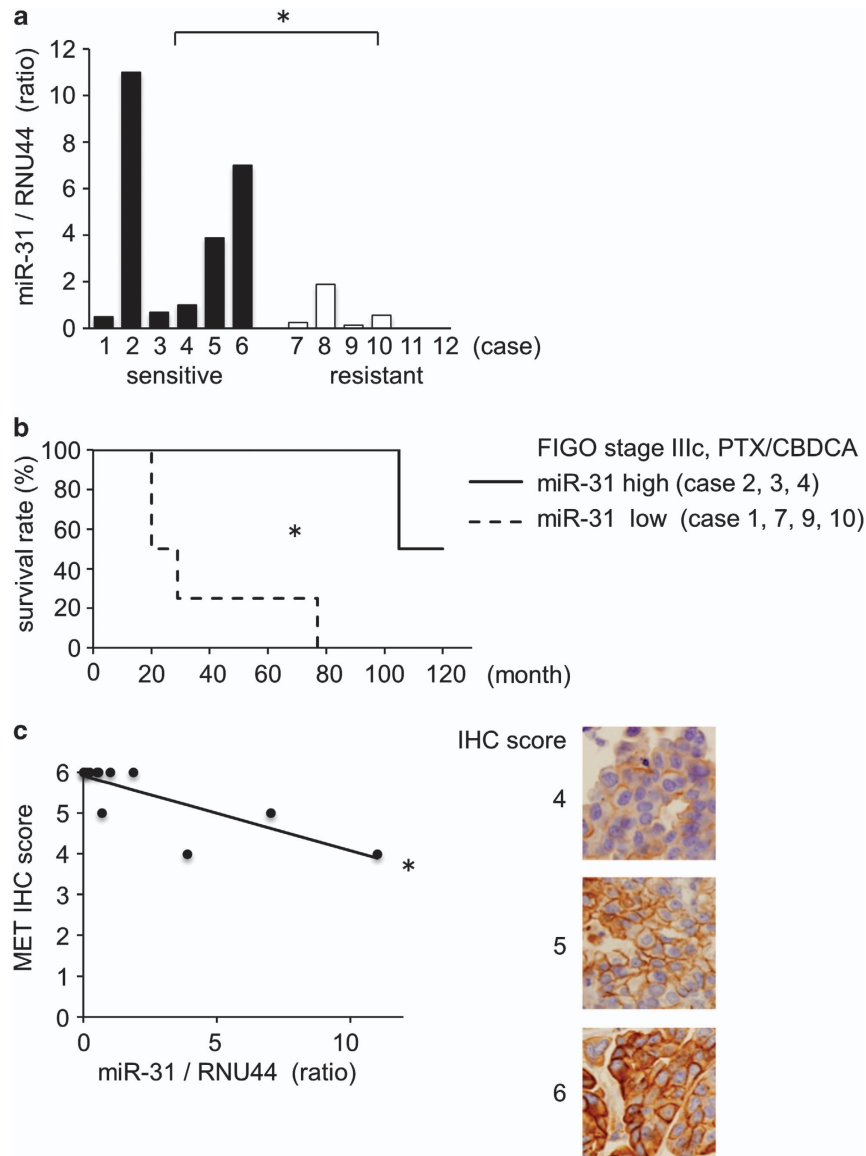


Figure 5. miR-31 expression decreased with chemosensitivity to PTX in human ovarian cancers. **(a)** Expression levels of miR-31 in human ovarian cancers were analyzed by real-time PCR. Cases 1–6 are chemosensitive and cases 7–12 are chemoresistant to taxane/platinum reagents. $*P < 0.05$, unpaired one-tailed *t*-test. **(b)** Prognosis of patients of ovarian cancers classified as miR31-high (solid line) and miR31-low (broken line) group. Kaplan–Meier curves for seven FIGO stage IIIc human primary ovarian cancers depicting overall survival, stratified based on miR-31 level. $*P < 0.05$, log-rank test. CBDCA, carboplatin; PTX, paclitaxel. Median follow-up = 67 months. **(c)** Correlation of expression levels of miR-31 and immunohistochemical reactivity of MET. IHC score, immunohistochemistry score. Representative results of IHC with scores 4, 5 and 6 are shown as photographs, $\times 400$; $*P < 0.05$, single regression analysis.

AG490 (Calbiochem) and proteasome inhibitor MG132 (Sigma), were dissolved in dimethyl sulfoxide (DMSO). Recombinant human hepatocyte growth factor (HGF) (Peprotech, Rocky Hill, NJ, USA) was dissolved in double distilled water (DDW) with 0.9% NaCl. Carboplatin, doxorubicin and gemcitabine (Sigma) were dissolved in DDW. Cycloheximide (CHX) (Sigma) was dissolved in ethanol (EtOH).

The MTT assay was performed for drug sensitivity assays using Cell Proliferation Kit I (Roche, Mannheim, Germany) according to the manufacturer's instructions. Briefly, 1.0×10^4 cells were seeded onto 96-well plates in 100 μ l culture medium with reagents. An equal volume of DMSO was used as control. The wavelength to measure absorbance of the formazan product was 570 nm, and the reference wavelength was 690 nm.

MicroRNA microarray

Microarray analyses were performed as previously described.⁴⁵ Total RNA was isolated from KFr13 and KFr13Tx by using RNeasy Mini Kit (Qiagen, Tokyo, Japan) according to the manufacturer's protocol. In brief, 50 μ g of

total RNA was enriched for the specimens of small amount of RNA, tailed by using the mirVana miRNA Labeling kit (Ambion, Austin, TX, USA), and fluorescently labeled by using amine-reactive Cy5 dyes (Amersham Pharmacia, Piscataway, NJ, USA). The fluorescence-labeled RNAs were hybridized for 16 h with miRNA array slides. Microarrays were performed using mirVanaTM miRNA Bioarray V2 (Ambion) and scanned by GenePix 4000B (Molecular Devices Inc., Sunnyvale, CA, USA). This microarray carries genes for a total 633 kinds of miRNAs containing 328 human genes, 238 rat genes and 266 mice, with each gene spotted in quadruplicate. Raw data were normalized and analyzed using Array ProTM Analyzer Ver4.5 (Media Cybernetics Inc., Rockville, MD, USA). Analyzed data were selected by using MicroArray Data Analysis Tool (Filgen Inc., Nagoya, Japan).

Overexpression of miR-31

Pre-miR-31 was transfected into KFr13Tx using BLOCK-iT Lentiviral miR RNAi Expression System (Invitrogen, Carlsbad, CA, USA) following the manufacturer's protocol. The sequences for miR-31 precursor (pre-miR-31)

were as follows: forward 5'-TGCTGGGAGAGGAGGCAAGATGCTGGCATAGCT GTTGAACCTGGGAACCTGCTATGCCAACATATTGCCATCTTTCC-3' and reverse 5'-CCTGGGAAAGATGGCAATATGTTGGCATAGCAGGTTCCAGTTCAACAGCT ATGCCAGCATCTTGCTCTCTCCC-3'. pcDNATM6.2-GW/EmGFP-miR plasmid (Invitrogen) was used as a negative control (mock). We repeated blasticidin selection at a concentration of 15–90 µg/ml and obtained three clones with different miR-31 expression. Total RNA was extracted by using TRIzol Reagent (Invitrogen). miR-31 was quantified by quantitative real-time PCR using TaqMan MicroRNA Reverse Transcription Kit (Applied Biosystems, Foster City, CA, USA) and TaqMan MicroRNA Assays (Applied Biosystems) according to manufacturer's instructions. We assessed miRNA expression by relative quantification using the $2^{-\Delta\Delta C_t}$ method⁴⁶ to determine fold changes in expression. The small nucleolar RNA RNU44 served as an endogenous control.

Inhibition of translation and of proteasome activity

Cells with ~80% confluence in 6-well plate were pretreated with 10 µg/ml of CHX to prevent *de novo* synthesis of MET for 4 h, or 0, 10 and 15 µM of MG132 to inhibit proteasome for 4 h. Equal volume of EtOH or DMSO were used as controls.

Luciferase reporter assay

Luciferase vectors (Genecopoeia, Rockville, MD, USA) were employed. The wild-type (NM_000245.2) or mutant MET 3'-UTR sequence was inserted into downstream of the firefly luciferase reporter gene, which was controlled by the SV40 enhancer for expression in mammalian cells (Genecopoeia, HmiT011181-MT01, HmiT011181-MT01-02), whereas no oligonucleotides were inserted in control vector (Genecopoeia, CmiT000001-MT01). Renilla luciferase was used as a tracking indicator for successful transfection. KFr13Tx mock and miR-31 cells with 80% confluence in 6-well plate were transfected with 2 µg of each vector using Lipofectamine 2000 (Invitrogen). Cells were harvested after 48 h and lysed with passive lysis buffer (Promega, Madison, WI, USA). Luciferase activity was measured by a dual luciferase reporter assay system (Promega). Firefly luciferase activities were normalized by the Renilla luciferase activity.

Cloning of target mRNA in miRNA–mRNA–Argonaute2 (Ago2) complex

miRNA–mRNA–Ago2 complex was immunoprecipitated from 7.0×10^6 cells of KFr13Tx mock and KFr13Tx miR-31 using microRNA Isolation Kit, Human Ago2 (Wako, Osaka, Japan), then cDNA amplification from mRNA in miRNA–mRNA–Ago2 complex was performed using Target mRNA Cloning Kit (Wako). PCR amplification of MET 3'-UTR was performed using GoTaq Green Master Mix (Promega). miR-31 in miRNA–mRNA–Ago2 complexes of both cell lines were also quantitatively measured by real-time PCR.

RNA interference for MET

Three siRNAs against MET (Thermo Fisher Scientific, Waltham, MA, USA) and non-targeting siRNA (Thermo Scientific Dharmacon) were transfected into KFr13Tx cells by using HiPerFect transfection reagent (Qiagen) in six-well plate. Cells were harvested and lysed after 48 h.

miRNA inhibitor

Two hundred and fifty nanomolar miRIDIAN microRNA hairpin inhibitor and its negative control (Thermo Scientific Dharmacon) were employed to transiently inhibit miR-31 and transfected 48 h before seeding with Oligofectamine (Invitrogen).

Immunoblotting

Cells were lysed with lysis buffer (10 mM Tris–HCl (pH 7.4), 150 mM NaCl, 1 mM EDTA, 0.5% NP40, 50 mM NaF, 1 mM phenylmethylsulfonyl fluoride, 1 mM Na₃VO₄). Proteins were separated by SDS–polyacrylamide gel electrophoresis and transferred onto a polyvinylidene difluoride filter (Millipore, Billerica, MA, USA) by standard method. Filters were incubated with rabbit polyclonal antibody against MET (Santa Cruz Biotechnology), and mouse monoclonal antibodies against p53 (Dako, Glostrup, Denmark), actin (Millipore) or α -tubulin (Santa Cruz Biotechnology) were incubated overnight at 4 °C, and then with peroxidase-labeled secondary antibodies for 1 h. Proteins were visualized by Novex ECL Chemiluminescent Substrate

Reagent Kit (Invitrogen) and quantified using a Lumino Image Analyzer (LAS1000, Fuji Film, Tokyo, Japan).

Reverse transcription PCR

Total RNA was extracted by using TRIzol Reagent (Invitrogen), and reverse transcription was performed using SuperScript II Reverse Transcriptase (Invitrogen) following the manufacturer's instruction. The PCR amplification was performed using GoTaq Green Master Mix (Promega). Primers used for expression analysis were as following: pre-miR31—sense, 5'-GGAGAGGAGGCAAGATGCTG-3'; pre-miR31—antisense, 5'-GGAAAGATG GCAATATGTTG-3'; glyceraldehyde-3-phosphate dehydrogenase (GAPDH)—sense, 5'-CTCATGACCACAGTCCATGC-3'; GAPDH—antisense, 5'-TTACTC CTTGGAGGCCATGT-3'; MET—sense, 5'-GGTGAAGTGTTAAAAGTTGGA-3'; MET—antisense, 5'-ATGAGGAGTGTGACTCTTG-3'; MET 3'-UTR—sense, 5'-TTGAGTTGGCTGTTGTTGC-3'; MET 3'-UTR—antisense, 5'-CCTGTTGAT GGGATGTTCC-3'.

Human ovarian tumors

Tumor specimens from patients with ovarian cancer were obtained from Hokkaido University Hospital under institutional review board-approval. Informed consent was obtained from each patient. Patients treated at Hokkaido University Hospital between 1999 and 2010 were eligible. All samples were obtained at the initial surgery. miRNA was extracted by RecoverAllITM Total nucleic Acid Isolation Kit (Ambion) from formalin-fixed, paraffin-embedded tissues, of which epithelial tumors were confirmed by microscopical examination, and miR-31 was detected by quantitative real-time PCR described above.

Immunohistochemistry

The formalin-fixed, paraffin-embedded tissues were used for detection of MET expression. The sections were incubated with anti-MET rabbit monoclonal antibody (EP1454Y) (Abcam, Cambridge, UK) with 1:250 dilution. All of the slides were reviewed by three full-boarded pathologists without knowledge of the clinical data. Immunohistochemical positivities were evaluated by proportion and intensity. For analysis of proportion, four tired evaluation was applied as 0 to 3; as no staining (0), 1–10% (1), 11–50% (2) and 51–100% of tumor cells (3). For evaluation of intensity, there are following four criteria: as negative (0), weak (1), intermediate (2) and strong (3). MET immunohistochemistry score was shown as sum of proportional and intensity scores (0 to 6).

Analysis of tumor-forming potential *in vivo*

All experiments were conducted in accordance with guidelines authorized by the Animal Research Committee Hokkaido University. Six-week-old BALB/c nude mice (Clea, Tokyo, Japan) were injected subcutaneously into their flanks with 2×10^7 KFr13Tx mock or KFr13Tx miR-31 cells in 200 µl of matrigel (BD Biosciences, San Jose, CA, USA) and 50 µl of normal culture medium. PTX and/or SU11274 was administered intraperitoneally at 10 mg/kg, respectively, in 300 µl of normal culture medium on day 1. All mice were killed on day 28 and tumor weight was measured. In another experiment, six-week-old BALB/c nude mice were intraperitoneally injected with 2×10^7 KFr13Tx mock or miR-31 cells. PTX was administered intraperitoneally at 10 mg/kg with or without 3 µM of SU11274, respectively, in 300 µl of normal culture medium on day 1 or weekly (days 7, 14 and 21).

Statistical analysis

Data were presented as mean \pm s.e.m., and unpaired two-tailed Student's *t*-test was used for comparisons, with $P < 0.05$ considered significant.

CONFLICT OF INTEREST

The authors declare no conflict of interest.

ACKNOWLEDGEMENTS

We thank Professor Yoshihiro Kikuchi (National Defense Medical College, Saitama, Japan) for human KFr13 ovarian cancer cells. We also thank Kigawa and Dr Hiroaki Itamochi (Tottori University School of Medicine) for human KF and TU-OM-1 ovarian cancer cells. This work was supported in part by Grants-in-Aid for Scientific Research from the Ministry of Education, Culture, Sports, Science and Technology (MEXT) of Japan (HW for Scientific Research C 22591844, and ST for Scientific Research B

70261287), and from the Japan Society for the Promotion of Science, and from the Ministry of Health, Labor, and Welfare of Japan.

REFERENCES

- Boyle P, Levin B. *World cancer report 2008*. World Health Organization: Lyon, 2008, 2008.
- Landis SH, Murray T, Bolden S, Wingo PA. Cancer statistics, 1999. *CA Cancer J Clin* 1999; **49**: 8–31.
- Cannistra SA. Cancer of the ovary. *N Engl J Med* 2004; **351**: 2519–2529.
- Kristensen GB, Trope C. Epithelial ovarian carcinoma. *Lancet* 1997; **349**: 113–117.
- Vaughan S, Coward JI, Bast Jr RC, Berchuck A, Berek JS, Brenton JD *et al*. Rethinking ovarian cancer: recommendations for improving outcomes. *Nat Rev Cancer* 2011; **11**: 719–725.
- Bartel DP. MicroRNAs: target recognition and regulatory functions. *Cell* 2009; **136**: 215–233.
- Calin GA, Dumitru CD, Shimizu M, Bichi R, Zupo S, Noch E *et al*. Frequent deletions and down-regulation of micro-RNA genes miR15 and miR16 at 13q14 in chronic lymphocytic leukemia. *Proc Natl Acad Sci USA* 2002; **99**: 15524–15529.
- Volinia S, Calin GA, Liu CG, Ambs S, Cimmino A, Petrocca F *et al*. A microRNA expression signature of human solid tumors defines cancer gene targets. *Proc Natl Acad Sci USA* 2006; **103**: 2257–2261.
- Garzon R, Marcucci G, Croce CM. Targeting microRNAs in cancer: rationale, strategies and challenges. *Nat Rev Drug Discov* 2010; **9**: 775–789.
- Zhou M, Liu Z, Zhao Y, Ding Y, Liu H, Xi Y *et al*. MicroRNA-125b confers the resistance of breast cancer cells to paclitaxel through suppression of pro-apoptotic Bcl-2 antagonist killer 1 (Bak1) expression. *J Biol Chem* 2010; **285**: 21496–21507.
- Fornari F, Milazzo M, Chieco P, Negrini M, Calin GA, Grazi GL *et al*. MiR-199a-3p regulates mTOR and c-Met to influence the doxorubicin sensitivity of human hepatocarcinoma cells. *Cancer Res* 2010; **70**: 5184–5193.
- Yang N, Kaur S, Volinia S, Greshock J, Lassus H, Hasegawa K *et al*. MicroRNA microarray identifies Let-7i as a novel biomarker and therapeutic target in human epithelial ovarian cancer. *Cancer Res* 2008; **68**: 10307–10314.
- Valastyan S, Reinhardt F, Benaich N, Calogrias D, Szasz AM, Wang ZC *et al*. A pleiotropically acting microRNA, miR-31, inhibits breast cancer metastasis. *Cell* 2009; **137**: 1032–1046.
- Jeffers M, Taylor GA, Weidner KM, Omura S, Vande Woude GF. Degradation of the Met tyrosine kinase receptor by the ubiquitin-proteasome pathway. *Mol Cell Biol* 1997; **17**: 799–808.
- Ciechanover A, Shkedy D, Oren M, Bercovich B. Degradation of the tumor suppressor protein p53 by the ubiquitin-mediated proteolytic system requires a novel species of ubiquitin-carrier protein, E2. *J Biol Chem* 1994; **269**: 9582–9589.
- Benedet JL, Bender H, Jones 3rd H, Ngan HY, Pecorelli S. FIGO staging classifications and clinical practice guidelines in the management of gynecologic cancers. FIGO Committee on Gynecologic Oncology. *Int J Gynaecol Obstet* 2000; **70**: 209–262.
- Eisenhauer EA, Therasse P, Bogaerts J, Schwartz LH, Sargent D, Ford R *et al*. New response evaluation criteria in solid tumours: revised RECIST guideline (version 1.1). *Eur J Cancer* 2009; **45**: 228–247.
- van der Burg ME, van Lent M, Buyse M, Kobierska A, Colombo N, Favalli G *et al*. Gynecological Cancer Cooperative Group of the European Organization for Research and Treatment of Cancer. The effect of debulking surgery after induction chemotherapy on the prognosis in advanced epithelial ovarian cancer. *N Engl J Med* 1995; **332**: 629–634.
- Eisenkop SM, Spirtos NM. What are the current surgical objectives, strategies, and technical capabilities of gynecologic oncologists treating advanced epithelial ovarian cancer? *Gynecol Oncol* 2001; **82**: 489–497.
- Horwitz SB. Mechanism of action of taxol. *Trends Pharmacol Sci* 1992; **13**: 134–136.
- Wahl AF, Donaldson KL, Fairchild C, Lee FY, Foster SA, Demers GW *et al*. Loss of normal p53 function confers sensitization to Taxol by increasing G2/M arrest and apoptosis. *Nat Med* 1996; **2**: 72–79.
- Patel N, Chatterjee SK, Vrbanac V, Chung I, Mu CJ, Olsen RR *et al*. Rescue of paclitaxel sensitivity by repression of Prohibitin1 in drug-resistant cancer cells. *Proc Natl Acad Sci USA* 2010; **107**: 2503–2508.
- Tan M, Jing T, Lan KH, Neal CL, Li P, Lee S *et al*. Phosphorylation on tyrosine-15 of p34(Cdc2) by ErbB2 inhibits p34(Cdc2) activation and is involved in resistance to taxol-induced apoptosis. *Mol Cell* 2002; **9**: 993–1004.
- Goncalves A, Braguer D, Kamath K, Martello L, Briand C, Horwitz S *et al*. Resistance to Taxol in lung cancer cells associated with increased microtubule dynamics. *Proc Natl Acad Sci USA* 2001; **98**: 11737–11742.
- Lu J, Tan M, Huang WC, Li P, Guo H, Tseng LM *et al*. Mitotic deregulation by survivin in ErbB2-overexpressing breast cancer cells contributes to Taxol resistance. *Clin Cancer Res* 2009; **15**: 1326–1334.
- Kavallaris M, Kuo DY, Burkhart CA, Regl DL, Norris MD, Haber M *et al*. Taxol-resistant epithelial ovarian tumors are associated with altered expression of specific beta-tubulin isotypes. *J Clin Invest* 1997; **100**: 1282–1293.
- Gottesman MM, Pastan I, Ambudkar SV. P-glycoprotein and multidrug resistance. *Curr Opin Genet Dev* 1996; **6**: 610–617.
- Valeri N, Gasparini P, Braconi C, Paone A, Lovat F, Fabbri M *et al*. MicroRNA-21 induces resistance to 5-fluorouracil by down-regulating human DNA MutS homolog 2 (hMSH2). *Proc Natl Acad Sci USA* 2010; **107**: 21098–21103.
- Sarver AL, Li L, Subramanian S. MicroRNA miR-183 functions as an oncogene by targeting the transcription factor EGR1 and promoting tumor cell migration. *Cancer Res* 2010; **70**: 9570–9580.
- Miller TE, Ghoshal K, Ramaswamy B, Roy S, Datta J, Shapiro CL *et al*. MicroRNA-221/222 confers tamoxifen resistance in breast cancer by targeting p27Kip1. *J Biol Chem* 2008; **283**: 29897–29903.
- Nakajima G, Hayashi K, Xi Y, Kudo K, Uchida K, Takasaki K *et al*. Non-coding microRNAs hsa-let-7g and hsa-miR-181b are associated with chemoresistance to 5-FU in colon cancer. *Cancer Genomics Proteomics* 2006; **3**: 317–324.
- Dai Y, Xie CH, Neis JP, Fan CY, Vural E, Spring PM. MicroRNA expression profiles of head and neck squamous cell carcinoma with docetaxel-induced multidrug resistance. *Head Neck* 2011; **33**: 786–791.
- Creighton CJ, Fountain MD, Yu Z, Nagaraja AK, Zhu H, Khan M *et al*. Molecular profiling uncovers a p53-associated role for microRNA-31 in inhibiting the proliferation of serous ovarian carcinomas and other cancers. *Cancer Res* 2010; **70**: 1906–1915.
- Ivanov SV, Goparaju CM, Lopez P, Zavadi J, Toren-Haritan G, Rosenwald S *et al*. Pro-tumorigenic effects of miR-31 loss in mesothelioma. *J Biol Chem* 2010; **285**: 22809–22817.
- Liu CJ, Tsai MM, Hung PS, Kao SY, Liu TY, Wu KJ *et al*. miR-31 ablates expression of the HIF regulatory factor FIH to activate the HIF pathway in head and neck carcinoma. *Cancer Res* 2010; **70**: 1635–1644.
- Trusolino L, Bertotti A, Comoglio PM. MET signalling: principles and functions in development, organ regeneration and cancer. *Nat Rev Mol Cell Biol* 2010; **11**: 834–848.
- Turke AB, Zejnullahu K, Wu YL, Song Y, Dias-Santagata D, Lifshits E *et al*. Pre-existence and clonal selection of MET amplification in EGFR mutant NSCLC. *Cancer Cell* 2010; **17**: 77–88.
- Suda K, Murakami I, Katayama T, Tomizawa K, Osada H, Sekido Y *et al*. Reciprocal and complementary role of MET amplification and EGFR T790M mutation in acquired resistance to kinase inhibitors in lung cancer. *Clin Cancer Res* 2010; **16**: 5489–5498.
- Bu R, Uddin S, Bavi P, Hussain AR, Al-Dayel F, Ghourab S *et al*. HGF/c-Met pathway has a prominent role in mediating antiapoptotic signals through AKT in epithelial ovarian carcinoma. *Lab Invest* 2011; **91**: 124–137.
- Tang MK, Zhou HY, Yam JW, Wong AS. c-Met overexpression contributes to the acquired apoptotic resistance of nonadherent ovarian cancer cells through a cross talk mediated by phosphatidylinositol 3-kinase and extracellular signal-regulated kinase 1/2. *Neoplasia* 2010; **12**: 128–138.
- Zihlhardt M, Park SM, Romero IL, Sawada K, Montag A, Krausz T *et al*. Foretinib (GSK1363089), an orally available multikinase inhibitor of c-Met and VEGFR-2, blocks proliferation, induces anoikis, and impairs ovarian cancer metastasis. *Clin Cancer Res* 2011; **17**: 4042–4051.
- Sawada K, Radjabi AR, Shinomiya N, Kistner E, Kenny H, Becker AR *et al*. c-Met overexpression is a prognostic factor in ovarian cancer and an effective target for inhibition of peritoneal dissemination and invasion. *Cancer Res* 2007; **67**: 1670–1679.
- Kikuchi Y, Miyauchi M, Kizawa I, Oomori K, Kato K. Establishment of a cisplatin-resistant human ovarian cancer cell line. *J Natl Cancer Inst* 1986; **77**: 1181–1185.
- Sato S, Itamochi H, Kigawa J, Oishi T, Shimada M, Sato S *et al*. Combination chemotherapy of oxaliplatin and 5-fluorouracil may be an effective regimen for mucinous adenocarcinoma of the ovary: a potential treatment strategy. *Cancer Sci* 2009; **100**: 546–551.
- Taganov KD, Boldin MP, Chang KJ, Baltimore D. NF-kappaB-dependent induction of microRNA miR-146, an inhibitor targeted to signaling proteins of innate immune responses. *Proc Natl Acad Sci USA* 2006; **103**: 12481–12486.
- Livak KJ, Schmittgen TD. Analysis of relative gene expression data using real-time quantitative PCR and the 2(-Delta Delta C(T)) Method. *Methods* 2001; **25**: 402–408.



Oncogenesis is an open-access journal published by Nature Publishing Group. This work is licensed under a Creative Commons Attribution-NonCommercial-ShareAlike 3.0 Unported License. To view a copy of this license, visit <http://creativecommons.org/licenses/by-nc-sa/3.0/>

Supplementary Information accompanies this paper on the Oncogenesis website (<http://www.nature.com/oncsis>).